The Monte Carlo Method: Versatility Unbounded in a Dynamic Computing World
Chattanooga, Tennessee, April 17-21, 2005, on CD-ROM, American Nuclear Society, LaGrange Park, IL (2005)

CORRELATED NEUTRON EMISSION IN FISSION WITH MONTE-CARLO METHODS

S. Lemaire, P. Talou, T. Kawano, M. B. Chadwick and D. G. Madland
Nuclear Physics group, Los Alamos National Laboratory, Los Alamos, NM, 87545
lemaire@lanl.gov; talou@lanl.gov; kawano@lanl.gov; mbchadwick@lanl.gov; dgm@lanl.gov

ABSTRACT

We have implemented a Monte-Carlo simulation of the statistical decay of fission fragments by sequential neutron emission. Within this approach, we calculate the center-of-mass and laboratory prompt neutron energy spectra as a function of fission fragment mass and as an integral over the whole mass distribution. We also assess the prompt neutron multiplicity distribution $P(\nu)$, both the average number of emitted neutrons and the average neutron energy as a function of the mass of the fission fragments (respectively $\bar{\nu}(A)$ and $\bar{\epsilon}(A)$). We calculate neutron-neutron correlations such as the full matrix $\bar{\nu}(A, TKE)$ as well as correlations between neutron energies. Two assumptions for partitioning the total available excitation energy among the light and heavy fragments are considered. Results are reported for the neutron-induced fission of ^{235}U (at 0.53 MeV neutron energy) and for the spontaneous fission of ^{252}Cf.

Key Words: neutron induced fission, spontaneous fission, neutron multiplicity, fission, correlations

1 INTRODUCTION

Following the fission of a heavy nucleus, two fragments are produced. Just after scission, these fragments, rich in neutrons, possess a given excitation energy that is then dissipated through the emission of so-called prompt fission neutrons and γ-rays until they reach their ground-state. They will then eventually undergo a β-decay, followed by the emission of so-called delayed neutrons. The main properties of the prompt fission neutrons, their average number $\bar{\nu}$ and their spectrum $N(\epsilon_n)$, are very important for numerous nuclear technologies.

From a theoretical point of view, the Los Alamos (or Madland-Nix) model [1] is commonly used to calculate these two physical quantities. With a few parameters fitted to experimental data, this model is able to accurately predict the spectrum $N(\epsilon_n)$ and the average number of prompt fission neutrons $\bar{\nu}$ as a function of the fissioning nucleus and its excitation energy.

However, the Los Alamos model can only calculate physical quantities averaged over many components, such as the fission fragments mass yields and the whole nuclear decay chain of a given fission fragment. More specific and exclusive information, e.g., the prompt neutron probability distribution $P(\nu)$ and neutron-neutron correlations, can not be obtained within this model. Emerging nuclear technologies could greatly benefit from knowing these quantities accurately. In addition, and more fundamentally, these observables are important to shed some light on the nuclear fission process itself. To go a step further than the Los Alamos model and predict these physical observables requires following in detail the fission fragment evaporation decay by sequential neutrons and γ-rays emission. The Monte Carlo method is perfectly adapted to such a task.

In this Proceeding, we present the work that we have initiated toward the development of a Monte Carlo simulation of the statistical decay of the fission fragments. In the first part, we will describe our theoretical model and the numerical methodology implemented in the Monte Carlo code. Numerical results for two different fissioning systems, namely the spontaneous fission of ^{252}Cf and the neutron-induced fission of ^{235}U, are presented in the following section, and compared to existing experimental data. A discussion of these preliminary results follows. As a conclusion, possible improvements of the current model and code are presented.

2 THEORETICAL APPROACH

In this work, we extend the Los Alamos model [1] by implementing a Monte-Carlo simulation of the statistical decay (Weisskopf-Ewing) of the fission fragments (FF) by sequential neutron emission. A Monte-Carlo approach leads to a much more detailed picture of the decay process and various physical quantities can then be assessed: the center-of-mass and laboratory prompt neutron energy spectrum $N(\epsilon_n)$, the prompt neutron multiplicity distribution $P(\nu)$, the average number of emitted neutrons and neutron energy as a function of the FF mass and total kinetic energy $\bar{\nu}(A, Z, TKE)$ and $\bar{\epsilon}(A, Z, TKE)$, and all possible neutron-neutron correlations.

Unlike in the Los Alamos model where many quantities are lumped together, our approach tries to follow in detail the statistical decay of the FF by sequential emission of individual neutrons. Many quantities and parameters, more or less known, enter as input in the calculation. We will now briefly describe the methodology used in the present work, and then go into some detail over the list of input quantities that enter in our calculations.

2.1 Methodology

A Monte Carlo approach allows following in detail any reaction chain and recording the result in a history-type file, which basically mimics the results of an experiment. A typical line of the history file contains: the initial fission fragment mass and charge, its initial excitation energy, and if any, the number and energy of neutrons emitted during the evaporation process. An analysis code (written in Perl) is then used to extract any information on distributions, correlations, spectra, etc. that can be inferred from the recorded information.

We first sample the FF mass and charge distributions, and pick a pair of light and heavy nuclei that will then decay by emitting zero, one or several neutrons. This decay sequence is governed by neutron emission probabilities at different temperatures of the compound nucleus and by the energies of the emitted neutrons.

The FF mass and charge distributions is given by $Y(A, Z) = Y(A)_{exp} \times P(Z)$, where $Y(A)_{exp}$ represents an experimental pre-neutron FF mass distribution. The charge distribution $P(Z)$ is assumed Gaussian in shape.

Of course, the particular decay path followed by this pair of nuclei depends on the available excitation energies, which can be deduced in the following manner. The total excitation energy available for the pair $(A, Z)_l$ (light), $(A, Z)_h$ (heavy) reads

$$E^*_T(A_l, A_h, Z_l, Z_h) = E^*_r(A_l, A_h, Z_l, Z_h) + B_n(A_c, Z_c) + e_n - TKE(A_l, A_h), \quad (1)$$

where $E_r^*(A_l, A_h, Z_l, Z_h)$ is the energy release in the fission process, which is given, in the case of binary fission, by the difference between the compound nucleus and the FF masses. $B_n(A_c, Z_c)$ and e_n are the separation and kinetic energies of the neutron inducing fission (in the case of spontaneous fission, both $B_n(A_c, Z_c)$ and e_n terms in Eq. (1) disappear). $TKE(A_l, A_h)$ is the total FF kinetic energy. In fact, TKE is not a single value but rather a distribution, assumed to be Gaussian, whose mean value and width are taken from experiment.

One of the long-standing questions about the nuclear fission process is how does the available total excitation energy get partitioned among the light and heavy fragments. In the present study, we have considered two hypotheses for partitioning this energy:

- Partitioning (H1) so that both light and heavy fragments share the same temperature (hypothesis identical to the one made in the Los Alamos model [1]) at the instant of scission. From this condition, it follows that the initial excitation energy of a given FF is:

$$E_{l,h}^* = E_T^* \frac{1}{1 + \frac{a_{h,l}}{a_{l,h}}}, \tag{2}$$

  where l and h refer to the light and heavy system.

- Partitioning (H2) using the experimental $\bar{\nu}(A)$ to infer the initial excitation of each fragment. This condition writes as follow:

$$E_{l,h}^* = E_T^* \frac{\bar{\nu}(A_{l,h})\langle\epsilon\rangle_{l,h}}{\sum\limits_{i=l,h} \bar{\nu}(A_i)\langle\epsilon\rangle_i}, \tag{3}$$

  where $\langle\epsilon\rangle_{l,h}$ is equal to the average energy removed per emitted neutron for a given fission fragment. It is the sum of the average center-of-mass energy of the emitted neutrons for a given FF ([8] and [9] for the neutron-induced fission (at 0.53 MeV) on ^{235}U and spontaneous fission of ^{252}Cf respectively) and of the average FF neutron separation energy.

Within the Fermi-gas model, the initial FF excitation energy $E_{l,h}^*$is simply related to the nuclear temperature $T_{l,h}$. The probability for the FF to emit a neutron at a given kinetic energy is obtained by sampling over the Weisskopf spectrum at this particular temperature [2] :

$$\phi(A, Z, \epsilon_n, T) = \frac{\epsilon_n}{T_{A,Z}^2} e^{\frac{-\epsilon_n}{T_{A,Z}}}, \tag{4}$$

where $T_{A,Z}$ is the nuclear temperature of the residual nucleus given by

$$T_{A,Z} = \sqrt{\frac{E^*(A, Z) - B_n(A, Z)}{a_{A-1,Z}}}, \tag{5}$$

with $a_{A,Z}$ the level density parameter of the nucleus.

The emission of a neutron of energy ϵ_n from the FF at the excitation energy E^* produces a residual nucleus with the excitation energy

$$E^*(A-1, Z) = E^*(A, Z) - \epsilon_n - B_n(A, Z). \tag{6}$$

The sequential neutron emission ends when the excitation energy of the residual nucleus is less than the sum of its neutron separation energy and pairing energy.

The transformation of the center-of-mass spectrum to the laboratory spectrum is done by assuming that neutrons are emitted isotropically in the center-of-mass frame of a FF. So, sampling over the angle of emission of the neutron $\theta_n \in [0, \pi]$ for each nucleus (A, Z), we infer the neutron energy in the laboratory frame, taking into account the recoil energy of the residual nucleus.

2.2 Input Parameters

The fission mass yields have been measured extensively and precisely for several nuclei and energies. In the present calculation, we sample over the pre-neutron fragments yields $Y(A)_{exp}$, i.e., before neutron evaporation, as reconstructed from the experimentally measured fission products mass distribution. In particular, we use the data by Hambsch [3] in the case of ^{252}Cf(sf), and the data by Schmitt [4] in the case of the neutron-induced fission (at 0.53 MeV) on ^{235}U.

255 fragments were used to represent the $Y(A, Z)$ for the neutron induced n(0.53 MeV)+^{235}U reaction. In particular, we considered 85 equispaced fragment masses (between $76 \leq A \leq 160$) with 3 isobars per fragment mass, around the most probable charge Z_p. In the case of spontaneous fission of ^{252}Cf, we used 315 FF between $74 \leq A \leq 178$ with 105 fragment masses.

Nuclear masses are used to calculate the energy release for a given pair of FF. It is a function of both mass and charge number of complementary fragments. The data tables by Audi, Wapstra, Thibault [5] were used in the present calculation.

We use in our calculation the level density parameter to be:

$$a(A, Z, U) = a^* \left\{ 1 + \frac{\delta W(A, Z)}{U} \left(1 - e^{-\gamma U} \right) \right\} \tag{7}$$

where $U = E^* - \Delta(A, Z)$, $\gamma = 0.05$, a^* is the asymptotic level density parameter [6]. The pairing Δ and shell correction δW energies for the FF were taken from the nuclear mass formula of Koura et al.[7]. The level density parameters a^* approximate to $A/7.25$.

The total kinetic energy is used to assess the total FF excitation energy distribution. It is assumed to be approximately Gaussian in shape with an average value and width taken from the experiment (Ref. [3] for spontaneous fission of ^{252}Cf and Ref. [4] for the neutron induced n(0.53 MeV)+^{235}U reaction).

For sake of simplicity, we have assumed no mass, charge or energy dependence of the cross section for the inverse process of compound nucleus formation. This approximation will be reviewed later on.

We have used the average number of emitted neutrons $\bar{\nu}(A)$ as a way of partitioning the total excitation energy distribution between the light and heavy fragment. For the spontaneous fission of ^{252}Cf we used data from Refs. [8]. For the neutron induced n(0.53 MeV)+^{235}U reaction, we used data from Ref. [9].

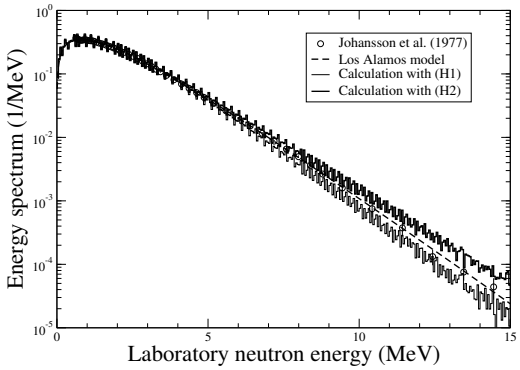

Figure 1: Neutron energy spectrum for n(0.53 MeV)+^{235}U reaction in the laboratory frame. The thick line is our Monte-Carlo calculation assuming partitioning of FF total excitation energy as a function of $\bar{\nu}_{exp}(A)$ (H2 hypothesis)and the thin line is the result obtained under the assumption of an equal temperature of complementary FF (H1 hypothesis). The dashed line is result of the Los Alamos model calculation using the optical model potential of Becchetti and Greenlees for the inverse process of compound nucleus formation.The experimental points are from Johansson and Holmqvist [10].

3 RESULTS AND DISCUSSION

Our Monte-Carlo simulations were done using 10^9 events for both spontaneous fission of ^{252}Cf and neutron induced n(0.53 MeV)+^{235}U reactions. Numerical results were obtained for various prompt fission neutron observables for the two energy partition hypotheses considered, (H1) and (H2).

For the neutron-induced reaction on ^{235}U, the neutron energy spectrum in the laboratory frames is shown in Fig. 1. Also shown for comparison are the results obtained with the Los Alamos model for the same reaction using the optical model potential of Becchetti and Greenlees for the average fragment of each peak. Experimental data points are taken from Johansson and Holmqvist [10]. The calculated spectrum obtained by assuming equal nuclear temperatures in both FF at scission is shown to be too soft when compared with experimental data, while the alternative hypothesis of splitting the energy according to $\bar{\nu}_{exp}(A)$ exhibits a much too hard spectrum.

The same conclusion can be drawn for ^{252}Cf (*sf*), although less pronounced that in the ^{235}U case.

Note that our Monte-carlo simulations assume a constant cross section for the inverse process of compound nucleus formation. It was shown in [1] that a more realistic Becchetti and Greenlees potential tends to lower the high energy tail of the spectra. The extension of our model to include a more realistic compound nucleus formation cross section is planned for the near future.

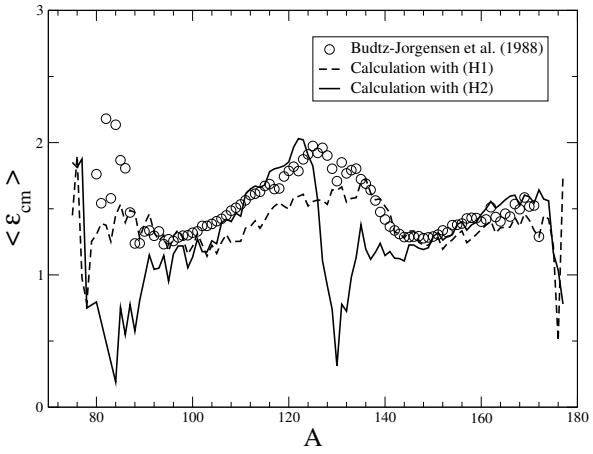

Figure 2: Average neutron emission energy, $\langle \epsilon_{cm} \rangle$, in the center of mass frame as a function of FF mass for ^{252}Cf (*sf*). The full points are experimental data from [8].

Experimentally [9], the average neutron energy emitted from the heavy fragment ($\langle \epsilon_h \rangle \sim 1.430$ MeV) is higher than the one emitted from the light fragment($\langle \epsilon_l \rangle \sim 1.330$ MeV). This observation is reproduced assuming the (H1) hyphothesis where $\langle \epsilon_h \rangle \sim 1.288$ MeV and $\langle \epsilon_l \rangle \sim 1.228$ MeV. On the contrary, for the (H2) case $\langle \epsilon_l \rangle \gg \langle \epsilon_h \rangle$ with 1.428 MeV$\gg 1.096$ MeV. This result is obtained for both studied reactions.

In addition to the calculated total neutron energy spectrum, we can investigate individual fragment spectra and extract from them an average center of mass neutron energy as a function of A. On Fig. 2, we compare the distribution of average neutron energies in the center of mass frame as a function of the FF mass number with experiments for ^{252}Cf (*sf*)[9]. The result obtained under the (H2) hypothesis agrees better with experiment in the mass region $\mathrm{A}_l \sim 105 - 124$ and $\mathrm{A}_h \sim 145 - 170$. Large deviations appear in the mass region $\mathrm{A}_l \sim 80 - 105$ and $\mathrm{A}_h \sim 124 - 144$. To understand this behaviour, we have to look at the inital excitation energy available in each fragment. In particular, it is interesting to note that the regions where deviations appear correspond to fragments with excitation energies of the order of the neutron separation energy ($E^*_{l,h} \sim 5 - 10$ MeV) or less. As noted by Weisskopf in Ref. [2], in this case, the probability of emitting a neutron is less than the one predicted by Eq.(4).

The result obtained under the (H1) hypothesis agrees with experiment on the heavy fragment mass region A$\sim 135 - 169$ but fails in the light fragment mass region A$\sim 96 - 135$.

The same conclusions but less pronounced are drawn for the neutron-induced reaction on ^{235}U.

The prompt neutron multiplicity distribution $P(\nu)$ can be inferred from our MC calculations, while most other approaches can only assess the average value of this distribution, $\bar{\nu}$.

To the best of our knowledge, only a limited number of experimental data exist for $P(\nu)$. Our

Fission reaction		$\bar{\nu}_l$	$\bar{\nu}_h$	$\bar{\nu}$	$\langle E_l^* \rangle$	$\langle E_h^* \rangle$
^{235}U+n(0.53 MeV)	H1	1.13	1.63	2.77	11.39	13.27
	H2	1.56	1.14	2.70	14.78	9.87
	Experiment[9]	1.42	1.01	-		
	Experiment[11]	-	-	2.47		
^{252}Cf (sf)	H1	1.76	2.44	4.19	16.50	18.94
	H2	2.18	1.91	4.09	20.22	15.04
	Experiment[12]	2.05	1.70	3.76		
	Experiment[11]	-	-	3.87		

Table I: Average prompt neutron multiplicities and initial excitation energies (in MeV).

numerical results are compared with the experimental distribution by Diven et al. [11] in Fig. 3 for ^{235}U. In both calculated cases (H1) and (H2), the average $\bar{\nu}$ of the distribution is larger than the experimental value. Average prompt neutron multiplicities for the light and heavy fragments are reported in Table I. Roughly speaking, the calculated $\bar{\nu}$ values are 10% higher than the experimental values. The dispersions of the calculated distributions are comparable to the experimental ones.

In the (H1) hypothesis of equal FF temperature at scission, the $\bar{\nu}$ value averaged over the heavy fragments yields is higher than the one for the light fragments, reflecting the higher average excitation energy available in the heavy fragments (cf Table I). In the (H2) calculation, the initial excitation energy partitioning is constrained by experimental $\bar{\nu}_{exp}$ values, thereby ensuring that the calculated ratio $\bar{\nu}_l/\bar{\nu}_h$ is very close to the experimental one.

A well known and important feature of prompt fission neutrons is the saw-tooth shape of the average number of emitted neutrons per fission as a function of the fragment mass. Experimental and calculated $\bar{\nu}$(A) distributions is shown in Fig. 4 for ^{252}Cf (*sf*). In both reactions studied, we expect the results under the (H2) assumption to be in better agreement with experiment as compared to the (H1) results. It is important to point out that the behaviour of this distribution around the symmetric fission, for both reactions studied, is mostly due to the overall constant value of the energy released in the fission $\langle E_r \rangle$ as a function of A and the increasing value of the average total fragment kinetic energy $\overline{TKE}$ as a function of the fragment mass. Also interesting, in the case of (H1) hypothesis, the increase of $\bar{\nu}$(A) around the masses 130 to 140 is essentially due to the drop of the average neutron binding energy $\langle B_n(A) \rangle$ in this mass region, allowing more

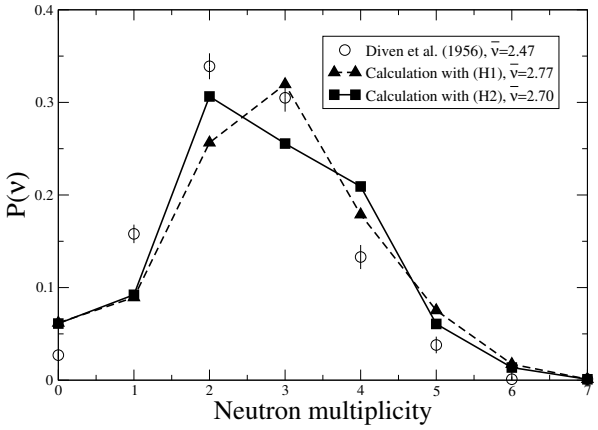

Figure 3: Neutron multiplicity distribution for n(0.53 MeV)+^{235}U reaction . Open square symbols are from our Monte-Carlo calculation assuming partitioning of FF total excitation energy as a function of $\bar{\nu}_{exp}(A)$ (H2 hypothesis), triangles are the result obtained under the assumption of an equal temperature of complementary FF (H1 hypothesis). The full points are experimental data from Diven et al. [11].

neutrons to be emitted due to the higher available excitation energy.

Another quantity of interest that has been measured for both reactions is the total average number of emitted neutrons as a function of the total kinetic energy. Our results are reported with experimental data on Fig. 5 for ^{235}U. The fact that in our approach the total excitation energy increase with decreasing TKE (see Eq.(1)) is responsible for the increase of $\bar{\nu}_{tot}$(TKE). In addition, since the same total excitation energy TXE is available whatever the partitioning is, similar results are obtained for the calculated $\bar{\nu}_{tot}$(TKE) under both (H1) and (H2) assumptions(Fig. 5).

Our calculations deviate from experimental results by overpredicting $\bar{\nu}_{tot}$ for low TKE (below 164 MeV for ^{235}U reactions). Some deviations also appear for higher TKE (above 179 MeV for ^{235}U reactions) where we predict too many prompt neutrons as compared to experimental data. In the particular case of neutron induced fission of ^{235}U a dramatic deviation between calculation and experiment on $\bar{\nu}_{tot}$ is observed for low TKE, that would indicate the presence of additional opened channels.

As pointed out earlier, knowledge only of $\bar{\nu}_{tot}$(TKE) cannot distinguish between the (H1) and (H2) hypotheses. However, one observable that would be sensitive to the partitioning of TXE is the distribution $\bar{\nu}$(A,TKE). Both measurements and calculations are compared on Fig. 6 for ^{235}U. Figure 6 shows some cuts of $\bar{\nu}$(A) versus TKE (for the following specific total kinetic energies 140, 145, 150, 155, 160 and 165 MeV). The comparison of our results with data on Fig. 6 clearly show different behaviours under (H1) and (H2) assumptions. The (H2) calculation is in better agreement with experimental points. However, some deviations are observed for mass numbers

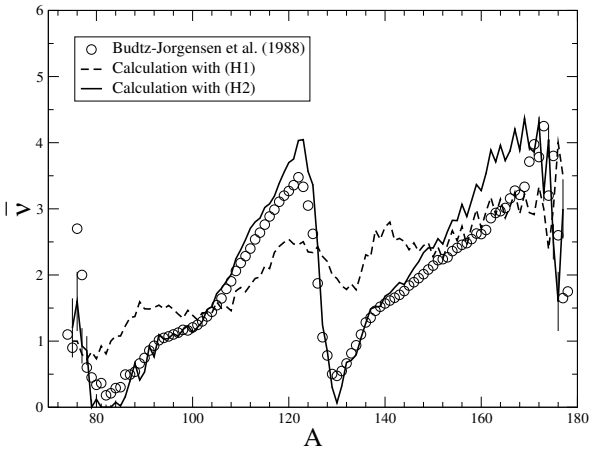

Figure 4: Average neutron multiplicity $\bar{\nu}$ as a function of the mass number of the FF for ^{252}Cf (*sf*). The full points are experimental data from [8].

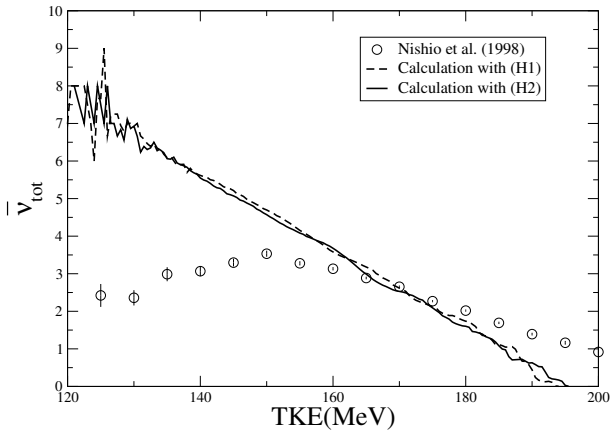

Figure 5: Sum of the neutron multiplicities from both FF plotted as a function of TKE for n(0.53 MeV)+^{235}U reaction. The full points are experimental data from [9].

A$\sim 101-102$ and A$\sim 105-106$ at low TKE (140, 145, 150 MeV), reflecting the observation made earlier on $\bar{\nu}_{tot}(TKE)$. In the particular region of total kinetic energy peak (TKE~ 165MeV), our calculation under the (H2) assumption is in fair agreement with experiment (Fig. 6).

4 CONCLUSION

In conclusion, we have developed a new and powerful tool to explore the process of neutron evaporation from the statistical decay of fission fragments. The choice of a Monte Carlo implementation to describe this decay process allows to infer important physical quantities that could not be assessed otherwise, for instance within the Los Alamos model framework. In particular, the multiplicity distribution of prompt neutrons $P(\nu)$, the distribution of ν as a function of the FF mass number and total kinetic energy, and neutron-neutron correlations can all be inferred from the present Monte-Carlo calculations.

We checked the sensitivity of our results upon the various parameters involved in the simulation. It appeared that the limit of the FF excitation energy beyond which no neutrons are emitted is of great importance. In particular, choosing this limit to be equal to the neutron separation energy plus pairing energy rather than just the neutron separation energy leads to much better results on neutron energy spectra and neutron multiplicity distributions for both hypotheses of partitioning the available total excitation energy. This condition impacts our calculation by lowering neutron emission at excitation energy close to the neutron separation energy thus reflecting the increasing competition with gamma ray emissions.

Our calculation is based on a Fermi-gas assumption $E^* = aT^2$. This leads to an overall too high nuclear temperature for low FF excitation energies. An improvement would be to add a constant temperature region to our description of neutron emission sequence for low FF excitation energies and keep the Fermi gas formulation for higher excitation energies. The investigation of the angular distribution of neutrons would be also an interesting extension of this work. Finally, the cross section for the inverse process of compound nucleus formation will be improved to include a neutron energy dependence.

This simulation tool can also be used to assess the validity of physical input assumptions, in particular the important question of how does the available total excitation energy get distributed among the light and heavy fission fragments.

Further progress of this work will help to shed some light on this question.

5 ACKNOWLEDGMENTS

We are grateful to Dr. F. S. Dietrich and Pr. T. Ohsawa for stimulating and encouraging discussions, Dr. F.-J. Hambsch and Dr. N. V. Kornilov for providing us with their experimental work.

6 REFERENCES

1. D. G. Madland, J. R. Nix, Nucl. Sci. Eng. **81** (1982) 213

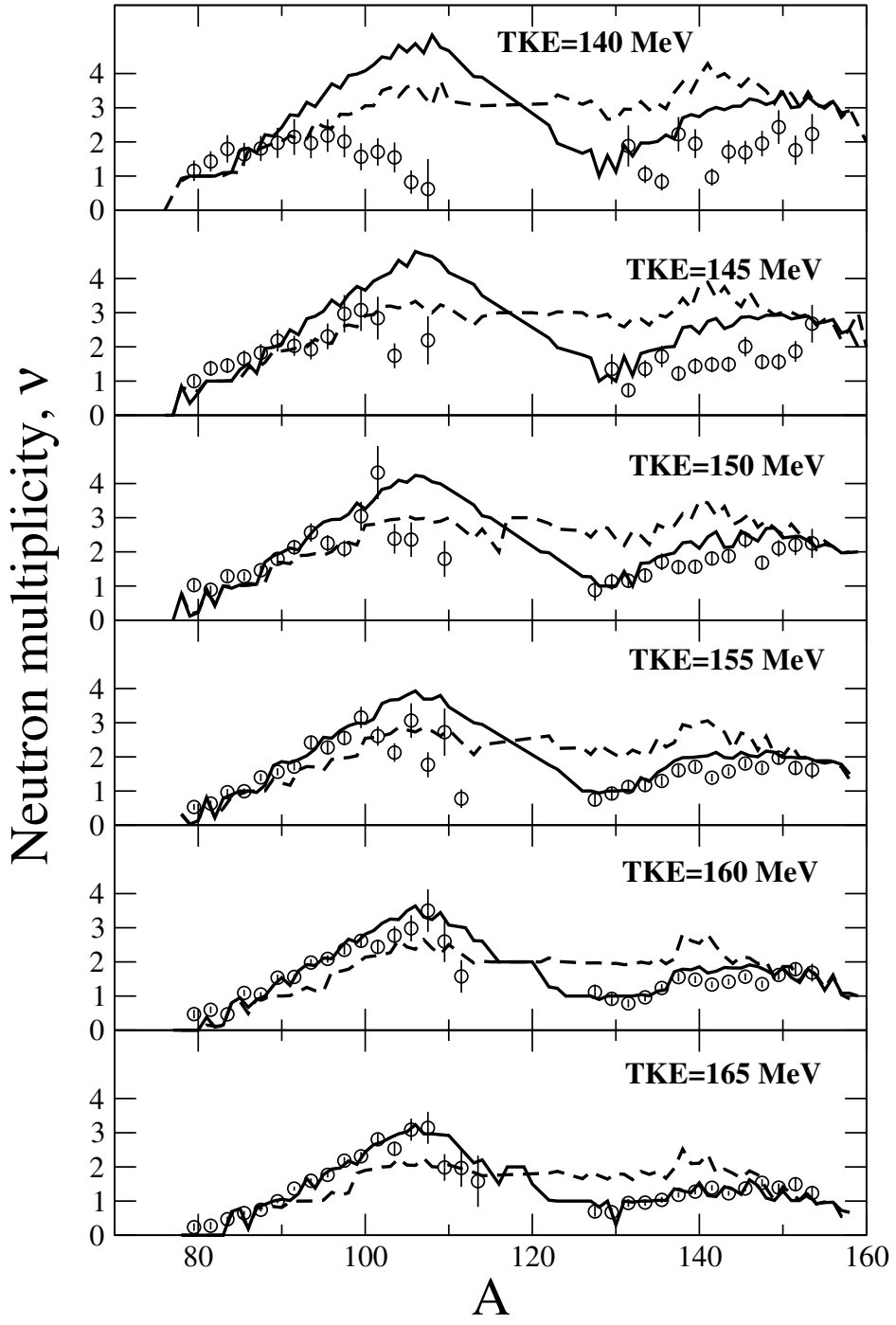

Figure 6: Average neutron multiplicity versus FF mass for specific 5 MeV TKE bins for n(0.53 MeV)+^{235}U reaction. The full points are experimental data from [9].

2. V. Weisskopf, Phys. Rev. **52** (1937) 295
3. F. J. Hambsch, S. Oberstedt, Nucl. Phys. **A617** (1997) 347
4. H. W. Schmitt, J. H. Neiler, F. J. Walter, Phys. Rev. **141** (1966) 1146
5. G. Audi, A. H. Wapstra, C. Thibault, Nucl. Phys. **A729** (2003) 337
6. A. V. Ignatyuk, K. K. Istekov, G. N. Smirenkin, Sov. J. Nucl. Phys., **29**, 450 (1979).
7. H. Koura, M. Uno, T. Tachibana, M. Yamada, Nucl. Phys., **A674**, 47 (2000); H. Koura, T. Tachibana, M. Uno, M. Yamada [private communication, 2004].
8. C. Budtz-Jørgensen, H. H. Knitter, Nucl. Phys. **A490** (1988) 307
9. K. Nishio, Y. Nakagome, H. Yamamoto, I. Kimura, Nucl. Phys. **A632** (1998) 540
10. P. I. Johansson and B. Holmqvist, Nucl. Sci. Eng. **62** (1977) 695
11. B. C. Diven, H. C. Martin, R. F. Taschek and J. Terrell, Phys. Rev. **101** (1956) 1012
12. A. S. Vorobyev, V. N. Dushin, F. J. Hambsch, V. A. Jakovlev, V. A. Kalinin, A. B. Laptev, B. F. Petrov, O. A. Shcherbakov, International Conference on Nuclear Data for Science & Technology, ND2004, Santa Fe, Sep. 26-Oct. 1 (2004).